Monthly Notices
of the
ROYAL ASTRONOMICAL SOCIETY

Mon. Not. R. Astron. Soc. **421,** 398–407 (2012) doi:10.1111/j.1365-2966.2012.20314.x

Gas and stellar metallicities in H II galaxies

P. Westera,[1,2]★ F. Cuisinier,[3]† D. Curty[2]★ and R. Buser[4]★

[1]*Universidade Federal do ABC, Rua Santa Adélia 166, 09.210-170 Santo André, SP, Brazil*
[2]*Observatório Nacional, Rua José Cristino 77, 20.921-400 Rio de Janeiro, RJ, Brazil*
[3]*Observatório do Valongo/UFRJ, Ladeira do Pedro Antônio 43, 20.080-090 Rio de Janeiro, RJ, Brazil*
[4]*Departement Physik, Universität Basel, Klingelbergstrasse 82, 4056 Basel, Switzerland*

Accepted 2011 December 1. Received 2011 November 26; in original form 2011 March 29

ABSTRACT

We examine the gas and stellar metallicities in a sample of H II galaxies from the Sloan Digital Sky Survey, which possibly contains the largest homogeneous sample of H II galaxy spectra to date.

We eliminated all spectra with an insufficient signal-to-noise ratio, without strong emission lines and without the [O II] λ3727 Å line, which is necessary for the determination of the gas metallicity. This excludes galaxies with redshift $\lesssim$0.033. Our final sample contains ∼700 spectra of H II galaxies.

Through emission line strength calibrations and a detailed stellar population analysis employing evolutionary stellar synthesis methods, which we already used in previous works, we determined the metallicities of both the gas and the stellar content of these galaxies.

We find that in H II galaxies up to stellar masses of $5 \times 10^9\,M_\odot$, enrichment mechanisms do not vary with galactic mass, being the same for low- and high-mass galaxies on average. They do seem to present a greater variety at the high-mass end, though, indicating a more complex assembly history for high-mass galaxies. In around 23 per cent of our H II galaxies, we find a metallicity decrease over the last few Gyr. Our results favour galaxy evolution models featuring constantly infalling low-metallicity clouds that retain part of the galactic winds. Above $5 \times 10^9\,M_\odot$ stellar mass, the retention of high-metallicity gas by the galaxies' gravitational potential dominates.

Key words: ISM: abundances – galaxies: abundances – galaxies: evolution – galaxies: starburst.

1 INTRODUCTION

H II galaxies are characterized by prominent emission lines. In fact, they are defined as having strong Hβ and O III lines, but other ionized hydrogen (Hα, Hγ, etc.) and high excitation metallicity lines (O II, N II and others) are strong too. These emission lines are driven by photoionization of interstellar gas by hot massive stars from young stellar populations (Sargent & Searle 1970; French 1980). The star-forming activity in H II galaxies is so strong that it can certainly not have been maintained at its present level during a Hubble time (see e.g. Searle, Sargent & Bagnuolo 1973). In fact, they are the most extreme case of star-forming galaxies, showing the highest excitation emission lines, and thus the highest (relative) star formation rates (SFRs).

They are also the lowest metallicity galaxies of the interstellar medium, with metallicities around one-tenth solar (Pérez-Montero & Díaz 2003; Vílchez & Iglesias-Páramo 2003; Kniazev et al. 2004; Izotov et al. 2006; Kehrig et al. 2006; Hägele et al. 2008; Pérez-Montero et al. 2010, and others).

It is now clear that the hypothesis of H II galaxies as galaxies experiencing their first star formation burst can be ruled out, and that their stellar content is predominantly old, older than 1 Gyr (Raimann et al. 2000; Cid Fernandes, Leão & Lacerda 2003; Kong et al. 2003; Westera et al. 2004; Asari et al. 2007; Cid Fernandes et al. 2007; Hoyos et al. 2007, and others). Nevertheless, both the high relative SFRs and the low metallicities indicate that H II galaxies are among the least evolved galaxies in existence, which assigns to them a special role as fossil record of galaxy evolution (Lequeux et al. 1979). They are, therefore, ideal objects for chemical evolution studies.

Several authors have developed theoretical evolutionary models of dwarf irregular galaxies, of which H II galaxies are a subcategory. Some of these models predict the galaxies' present-day stellar and gas metallicities, among other properties. In these models, several chemical enrichment processes are identified.

MacLow & Ferrara (1999) developed single-phased hydrodynamical models for dwarf galaxies. They model the effects of

★E-mail: pieter.westera@ufabc.edu.br, pieter@on.br (PW); curty@on.br (DC); Roland.Buser@unibas.ch (RB)
†In memoriam (1969–2011).

repeated Type II supernova (SNII) explosions from starbursts on the interstellar medium, i.e. the enrichment by the ejected metals on the one hand, and the gas loss by supernova winds on the other hand, taking into account the gravitational potential of their dark matter haloes. They find that, in galaxies with gas masses below $10^6\,M_\odot$, most of the gas is blown away, and in galaxies with masses between 10^7 and $10^9\,M_\odot$, mainly the newly formed metal-rich gas is blown away, whereas the already present, metal-poor, gas is retained. They do not calculate the final (present-day) metallicities of their model galaxies, but it is obvious that they remain low metallicity, at least the ones with gas masses below $10^9\,M_\odot$.

Recchi, Matteucci & D'Ercole (2001) and Recchi et al. (2002) simulate IZw18, one of the lowest metallicity galaxies known, using a single star formation burst model and a model with a doubly peaked star formation history. They use a lower SNII heating efficiency than MacLow et al. in their models, but include Type Ia supernovae (SNeIa), for which they use a higher heating efficiency. As a consequence, alpha elements are ejected less efficiently than in the MacLow et al. model, resulting in higher metallicities. The iron-peak elements, which are produced in SNeIa, on the other hand, are still ejected, causing high [α/Fe] ratios. The (gas) metallicity in their single burst model remains very low, [O/H] $\lesssim -1.3$, depending on the galaxy mass. In their (more likely) double burst model, [O/H] can reach values up to -1, depending on the details of the models, i.e. the stellar yields used, the stellar initial mass function (IMF), the time between the bursts, the duration of the second burst, the gas density and metallicity in the star-forming region, and the total mass of the stars formed in the second burst. The final metallicities of the double burst model galaxies are between 0.6 and 1 dex higher than after the first burst.

Tenorio-Tagle et al. (2006) include photoionization and cluster wind in their two-dimensional hydrodynamic calculations. They identify two mechanisms: the storage of clouds into a long-lasting ragged shell inhibiting the expansion of the thermalized wind and the steady filtering of the shocked wind gas through channels carved within the cloud layer. They conclude that both processes must be at work in H II galaxies. Unfortunately, they make no prediction about the present-day metallicity of their model galaxies.

In a series of papers, Recchi and collaborators use a new generation of chemo-dynamical models, some of which include infalling clouds. The first two, Recchi et al. (2004, 2006), are aimed at reproducing the properties of two specific objects, IZw18 and NGC1569, respectively. The third one, Recchi & Hensler (2007) investigates the influence of several factors, such as the cloudiness of the gas distribution, the IMF slope and stellar yields. They find that models with continuous low-level star formation periods in the past followed by a quiescent phase and a recent, stronger burst best reproduce the chemical properties of the studied galaxies. They also find that, for a homogeneous gas distribution, metals get blown away by galactic winds, but cool infalling intergalactic clouds can hamper these galactic winds. The final metallicities in the their various models vary from -2.5 to -0.8.

Although metallicity determinations of the various components of H II galaxies cannot discriminate how much each of these mechanisms contribute to the chemical evolution, they can quantify the metallicity at various stages of a galaxy's evolution, i.e. at the time of the formation of the old (>1 Gyr) stellar populations and at present, and thereby help to rule out some of the evolutionary scenarios, and support others. H II galaxies have the advantage that it is possible to determine independently the metallicities of the young and the old populations from their spectra. As the young populations were formed recently out of the same gas that is responsible for the emission lines, their metallicity can be assumed to be more or less the same as the one of the gas, which can be determined from the emission line strengths. The metallicity of the old populations, on the other hand, can be determined from the continuum and absorption features through population synthesis.

The main goal of the present work is to measure the chemical enrichment in a homogeneous sample of H II galaxies, and examine possible trends with galactic properties such as total mass. This way, we can evaluate the different models and make statements on the importance of the various enrichment mechanisms.

Until recently, the discovery of H II galaxies was limited to the visual inspection of objective-prism surveys, introducing ill-controlled biases and selection effects (for compilations, see Terlevich et al. 1991; Kehrig, Telles & Cuisinier 2004, and references therein).

The Sloan Digital Sky Survey (SDSS; York et al. 2000) presents for the first time a comprehensive data base of galactic spectra. Data release 7 (Abazajian et al. 2009) contains over 900 000 galaxy spectra that have been selected on clear magnitude limiting criteria. In an unprecedented manner, the SDSS allows us to study star-forming emission line galaxies based on clear and quantitative criteria, and not mere visual inspection.

In this work, we define clear emission line strength criteria to distinguish galaxies containing strongly excited gas from other emission line galaxies. We only include spectra that contain the [O II] λ3727 Å emission line, as this line is indispensable for an adequate determination of the gas metallicity. This criterion excludes galaxies with redshift $\lesssim$0.033. This way, we selected a homogeneous sample of $\sim$700 H II galaxy spectra of high quality from the SDSS.

In this sample, we determine the metallicities of both the gas and the old stellar content using emission line calibration and stellar population synthesis methods, respectively. It is the first time an independent metallicity determination of the gas and the stars is performed on a clearly defined H II galaxy sample.

The layout of this article is the following. In Section 2, the catalogue of spectra analysed in this work is presented. Section 3 gives a detailed description of the method we used to analyse the spectra. Subsection 3.1 describes how we determined the gas metallicity, and Section 3.2 is dedicated to the determination of the stellar metallicities. The main results are given in Section 4 and discussed in Section 5. A summary and the main conclusions can be found in Section 6.

2 THE DATA BASE

For this work, we used spectra from the SDSS Data Release 7, which have a signal-to-noise ratio (S/N) of S/N $> 4\,\mathrm{pixel}^{-1}$ at $m_g = 20.2$, but usually much higher, and cover a wavelength range 3800–9200 Å. Most important of all, it contains a large number of galaxy spectra, that is around 900 000.

Any analysis however relies on previous clear criteria to define what H II galaxies are. First, we rejected all spectra whose wavelength ranges do not include the region from 3677 to 3775 Å, which is needed to measure the [O II] λ3727 Å emission line strength, used in many strong line methods to determine the gas metallicity. This excludes galaxies with redshifts below 0.033. Another prerequisite for measuring this line strength is a sufficient S/N in this wavelength region. We only kept spectra with $\mathrm{S/N}_{[\mathrm{O\,II}]3727} \geq 2.8$. This criterion guarantees sufficiently low noise for the entire spectral range used in this work, since at longer wavelengths, the S/N of the spectra is higher than around the [O II] λ3727 Å line, i.e. $\gtrsim$8 in g.

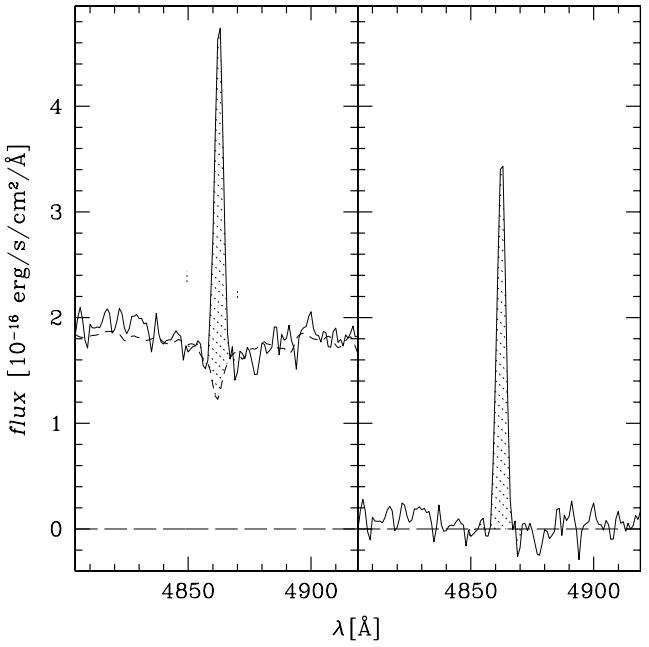

Figure 1. Illustration of the emission line strength measurement (here Hβ in 51957-0273-418). In the left-hand panel, the solid line represents the observed spectrum (rebinned to the BC03 wavelength grid), whereas the short-dashed line shows the best fit using the BC03 high-resolution library. The shaded region between these two lines shows the area used to calculate the emission line strength. The right-hand panel shows the emission line after subtracting the best fit. The shaded area corresponds to the shaded area between spectrum and best fit from the left-hand panel.

Table 1. Emission lines measured in this work.

Line	Central wavelength
[O II] λ3727 Å	3727 Å
Hϵ	3970 Å
Hδ	4102 Å
Hγ	4340 Å
[O III] λ4363 Å	4363 Å
[He II] λ4686 Å	4686 Å
Hβ	4861 Å
[O III] λ4959 Å	4959 Å
[O III] λ5007 Å	5007 Å
[He I] λ5876 Å	5876 Å
[O I] λ6300 Å	6300 Å
[S III] λ6312 Å	6312 Å
[N II] λ6548 Å	6548 Å
Hα	6563 Å
[N II] λ6584 Å	6584 Å
[S II] λ6717 Å	6717 Å
[S II] λ6731 Å	6731 Å
[O II] λ7319 Å	7319 Å
[O II] λ7330 Å	7330 Å

The spectra were then corrected for Galactic (foreground) gas extinction using the values given in the SDSS data base, which were derived from the Schlegel, Finkbeiner & Davis (1998) reddening maps. Using these extinction values and the Galactic extinction law of Fitzpatrick (1999), we dereddened the spectra. After that, we deredshifted them, and measured the emission line strengths.

In order to properly determine the emission line strengths, we first had to remove the contribution from the absorption lines of the underlying stellar populations. This was done by subtracting high-resolution spectra representing the stellar continuum from the empirical spectra as illustrated in Fig. 1. These high-resolution spectra were compiled by fitting the spectra of composite stellar populations, made up of three single stellar populations (SSPs), a young ($\leq$10 Myr), an intermediate age (20–500 Myr) and an old one (5 Gyr), from the 'BC03' integrated spectral energy distribution (ISED) library to the continua of the galaxy spectra. The 'BC03' library was produced using the Bruzual and Charlot (2003) Galaxy Isochrone Spectral Synthesis Evolution Library (GISSEL) code (Charlot & Bruzual 1991; Bruzual & Charlot 1993, 2003) implementing the Padova 1995 isochrones (Fagotto et al. 1994; Girardi et al. 1996) combined with the STELIB (Le Borgne et al. 2003) stellar library. Since it is made up of empirical high-resolution spectra, the 'BC03' library reproduces absorption line shapes well, and is ideal for this purpose. Table 1 lists all the lines we measured.

However, incomplete coverage of the stellar parameter space and calibration uncertainties of the STELIB library result in systematic errors in the overall spectral shapes. Therefore, the 'BC03' library is not a good choice for determining the properties of the stellar content from a full spectral fit. For the stellar population synthesis, we perform another fit using a different library, described in the next section.

Finally, we corrected the spectra for internal gas extinction using the Calzetti (2001) attenuation law. The extinction constants $E(B-V) = 0.44 \times 6.60 \log(I_{\mathrm{H}\alpha}/I_{\mathrm{H}\beta}/2.87)/4.04$ were estimated from the Hα/Hβ Balmer decrements following Calzetti (2001), adopting intrinsic ratios $I_{\mathrm{H}\alpha}/I_{\mathrm{H}\beta} = 2.87$ (Osterbrock 1989).

The factor of 0.44 stems from the correction for differential extinction between the stellar populations and the gas following Calzetti, Kinney & Storchi-Bergmann (1994). As our sample consists of H II galaxies only, which is a subclass of starburst galaxies, using this factor is justified. The emission line strengths were dereddened as well, using the same $E(B-V)$ values but without multiplying them by 0.44.

To make sure our sample contains only H II galaxies, we limited it to galaxies with strong emission lines at a high excitation level, by applying the two criteria:

$$\log\left(\frac{[\mathrm{O\,III}]\lambda5007\text{Å}}{\mathrm{H}\beta}\right) \geq 0.2 \parallel \log\left(\frac{[\mathrm{N\,II}]}{\mathrm{H}\alpha}\right) \leq -0.5, \qquad (1)$$

whereas [N II] = [N II] λ6548 Å + [N II] λ6584 Å. Of course, these criteria are more restrictive than the traditional definition of H II galaxies as galaxies showing strong Balmer lines. In fact, as our criteria are designed to identify galaxies with gas at a high excitation level, our sample is biased towards extreme case H II galaxies. As a consequence, we expect the galaxies of our sample to show typical properties of H II galaxies, but at a more pronounced level. For example, it consists of H II galaxies with low mass-to-light ratios and thus contains mainly dwarf galaxies. The reason for this approach, apart from emphasizing on typical H II galaxy properties, is to make sure that no 'contaminating' objects, such as low-ionization nuclear emission line regions (LINERs), enter the sample. Then, we separated the star-forming galaxies from active galactic nuclei (AGNs), using the Kewley et al. (2001) excitation line criterion,

$$\log\left(\frac{[\mathrm{O\,III}]\lambda5007\text{Å}}{\mathrm{H}\beta}\right) < \frac{0.61}{\log([\mathrm{N\,II}]/\mathrm{H}\alpha) - 0.47} + 1.19, \qquad (2)$$

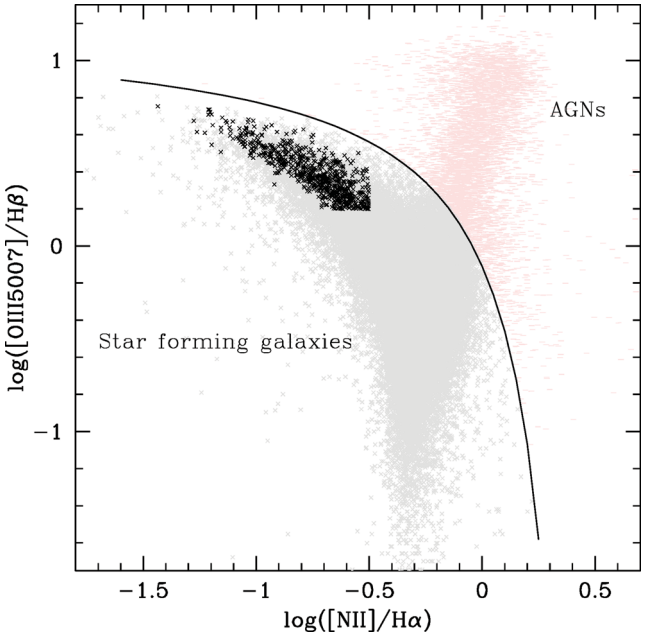

Figure 2. Excitation diagram for all galaxies of our sample (black crosses). The grey crosses represent the test sample, whereas galaxies identified as AGNs are shown as dashes. The solid line shows models from Kewley et al. (2001) used to separate the AGNs from star-forming galaxies.

as shown in Fig. 2.

Our final sample contains 712 H II galaxy spectra. The relatively low number of galaxies compared to the total number of over 900 000 galaxies in the SDSS Data Release 7 is due to our high requirements towards the quality of the spectra, and to the criterion that the spectra must contain all the lines necessary for our study. This way, we guarantee that the sample is not contaminated, and that the obtained results are trustworthy. However, the sample is large enough to be statistically significant.

We also defined a test sample, containing galaxies with some line emission, but not necessarily at a high level, that is Hα, Hβ, [O II] λ3727 Å, [O III] λ4959 Å, [O III] λ5007 Å, [N II] > 0. The reason for defining a test sample is, on the one hand, to identify properties typical of H II galaxies through comparison with the test sample and, on the other hand, to check our method, by comparing the results for our test sample with the ones obtained in other studies using similar galaxy samples. As we needed to measure the [O II] λ3727 Å line strength for the test sample as well, it is also limited to galaxies with redshift $\gtrsim$0.033. To guarantee sufficient quality, we applied the S/N criterion $S/N_g \geq 5$, where the S/N_g values were taken from the SDSS data base. Here too, we removed the AGNs using the Kewley et al. (2001) criterion. This way, our test sample contains 74 989 spectra. Given the criterion that the test sample galaxies show some line emission, it consists of star-forming galaxies, probably mostly spirals.

Fig. 2 shows both our sample of H II galaxies (in black) and the test sample (in grey) in a Baldwin–Phillips–Terlevich (BPT; Baldwin, Phillips & Terlevich 1981) classification diagram.

3 METHOD

3.1 Determination of the gas metallicities

We first measured the gas metallicity, which corresponds to the metallicity of the young stellar populations. In order to derive gas abundances from its line emission, hydrogen lines are needed, and the lines of at least one ion, generally oxygen, in its two dominant ionization stages. Unfortunately, the electron temperature method using the [O III] λ4363 Å emission line could not be used as this line and other auroral lines are much too weak to be measured with the necessary precision at the S/N values of the SDSS spectra. In most spectra, we do not even detect the [O III] λ4363 Å line at all. Hence, we are restricted to strong line methods. The [O II] λ7330 Å line could be used, but it is too sensitive to the electron temperature and is possibly 'contaminated' by recombination contributions.

We compare the gas metallicities derived from 11 different strong line methods.

A frequently used indicator is the [N II] λ6548 Å or the [N II] λ6584 Å line (Denicoló, Terlevich & Terlevich 2002; Pettini & Pagel 2004). However, since nitrogen is produced and destroyed during both primary and secondary nucleosynthesis, its abundance correlates in a non-evident way on (oxygen) metallicity. Therefore, it should be used only for rough estimates, to discriminate between the different branches of a multiple-valued method, for instance.

One such multiple-valued indicator is the R_{23} parameter (Pagel et al. 1979), which sums up the fluxes of the [O II] λ3727 Å and two strong [O III] lines, at 4959 and 5007 Å. As R_{23} is approximately proportional to the oxygen abundance at low metallicities, but decreases at high metallicities due to cooling, this indicator has a low- and a high-metallicity branch. In spite of this double valuedness, the R_{23} parameter is used in many metallicity calibrations (McGaugh 1991; Zaritsky et al. 1994; Pilyugin 2001a,b; Kewley & Dopita 2002; Kobulnicky & Kewley 2004; Pilyugin & Thuan 2005), some of which include a recipe, how to determine, on which branch a given galaxy lies, whereas others leave it up to the user to decide this. In one case, Zaritsky et al. (1994), a calibration is determined only for the high-metallicity branch. Another point that has to be taken into account (although in some methods this is ignored, i.e. Zaritsky et al. 1994) is that R_{23} depends not only on the metallicity of the ionized gas, but also on the hardness of the ionizing radiation, which can be quantified by the ionization parameter q, representing the ionizing photon flux per unit area divided by the number density of hydrogen atoms. Kewley & Dopita (2002) and Kobulnicky & Kewley (2004, 'new parametrization' and 'best estimate' methods) use the [O III]/[O II] ratio to calculate q in an iterative way from theory, and then determine [O/H] from R_{23} and q, whereas McGaugh (1991) uses the [O III]/[O II] ratio directly in an empirical calibration without determining q. In Pilyugin (2001a,b) and Pilyugin & Thuan (2005), the so-called excitation or ionization or, simply, P parameter is introduced for their empirical calibrations. It is defined as the [O III]/([O II]+[O III]) ratio, so the [O III]/[O II] ratio is related to it, $[O\,III]/[O\,II] = P/(1-P)$. Recapitulating, in all of these methods the gas metallicity is calculated from the R_{23} parameter and the [O III]/[O II] ratio.

Other strong line methods include Kobulnicky & Kewley (2004, [N II] method), combining the [N II] λ6584 Å line and the [O III]/[O II] ratio, and Pettini & Pagel (2004), employing the ratio between the [O III] λ5007 Å and [N II] λ6584 Å lines.

Fig. 3 shows the metallicities of our H II galaxy sample as determined by nine of the methods we studied, plotted against the ones determined by the 10th method, Pilyugin & Thuan (2005), which is the one we ended up adopting. The only calibration not shown here due to space limitations is the Pettini & Pagel (2004) [N II] one, which is a vertically squeezed and shifted downward version of the Denicoló et al. (2002) calibration (first panel).

Most methods yield similar relative metallicities, i.e. the methods agree upon the metallicity differences between galaxies. However,

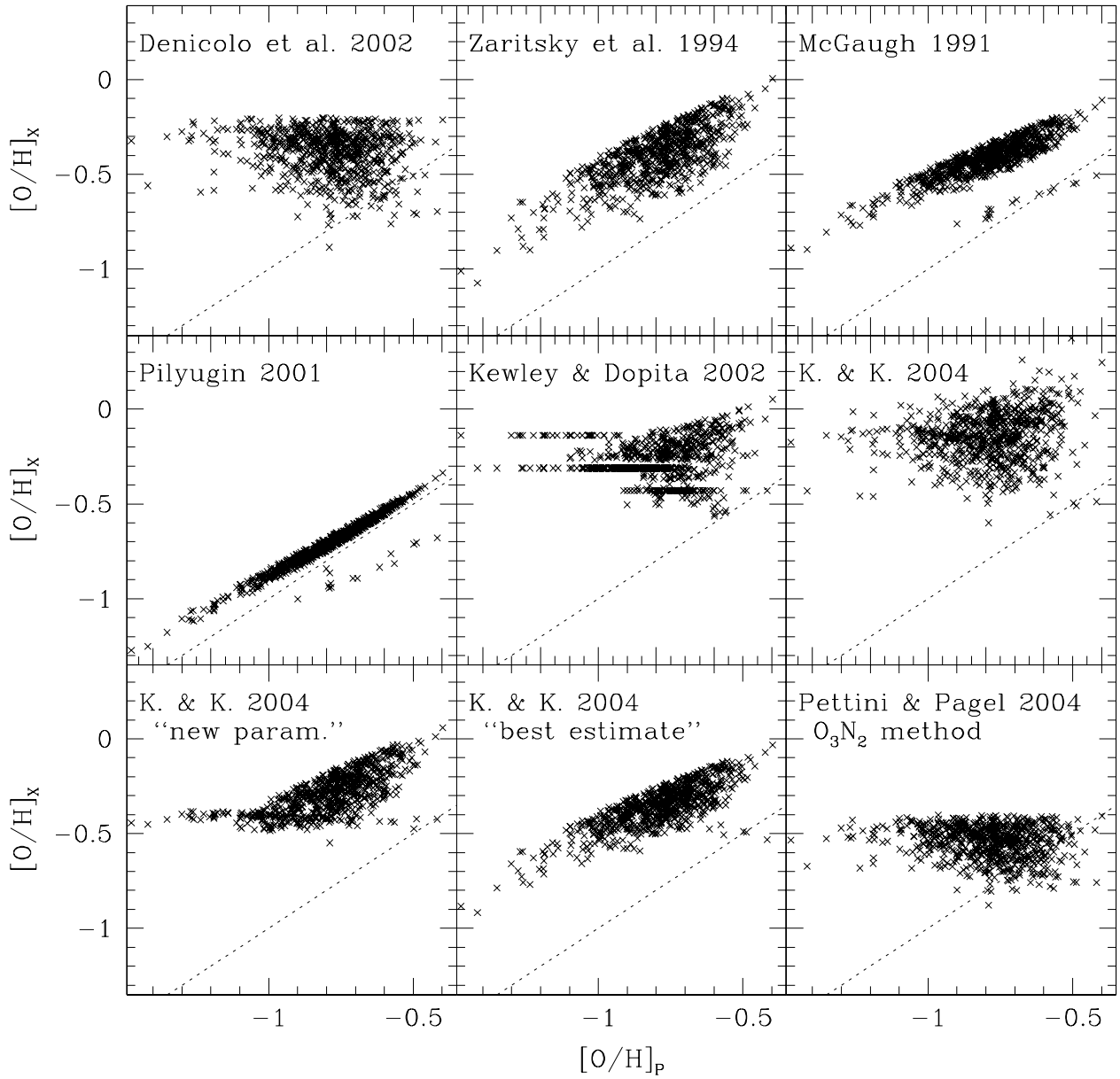

Figure 3. Comparison between the metallicities determined using the Pilyugin & Thuan (2005) method (*x*-axes) and the ones determined by nine other strong-line methods (*y*-axes). K. & K. 2004 stands for Kobulnicky & Kewley (2004). The dashed lines show unity, $[O/H]_X = [O/H]_P$. For further details, see text.

when it comes to absolute [O/H] values, systematic differences of up to 0.5 dex between methods can be observed. All methods apart from Pilyugin (2001a,b) and Pilyugin & Thuan (2005, *x*-axis) result in unrealistically high gas metallicities for H II galaxies. Especially the Kewley & Dopita (2002) and Kobulnicky & Kewley (2004) ones hardly ever give metallicities below −0.5. On top of that, the Kewley & Dopita (2002) and Kobulnicky & Kewley (2004, [N II] and 'new parametrization') methods did not always converge. The horizontal lines in the Kewley & Dopita (2002) panel are due to some cases, in which the expression $\log(O/H)+12=\frac{-k_1+\sqrt{k_1^2-4k_2(k_0-R_{23})}}{2k_2}$ gave complex values. In these cases, we used only the real part, $-k_1/2k_2$, which results in identical metallicity values for galaxies within the same ionization parameter range. When ignoring these galaxies, we obtain a similar relation as for the Kobulnicky & Kewley (2004) 'new parametrization of the Kewley & Dopita (2002)' method.

The method that yields the most realistic metallicities for the galaxies of our sample is the one by Pilyugin & Thuan (2005). It also accounts for the hardness of the ionizing radiation by means of the *P* parameter. Therefore, we adopted it for our gas metallicity determination. To determine on which branch a given galaxy lies, we used the metallicity estimate based on the [N II]λ6548Å/Hα ratio by Denicoló et al. (2002), as suggested by various authors (Pérez-Montero & Díaz 2005; Hoyos et al. 2007, and others). Most galaxies of our sample lie on the high-metallicity branch.

López-Sánchez & Esteban (2010) come to the same conclusion after comparing a series of empirical methods, like the ones presented in this section, with the results of the electron temperature method for a sample of 31 Wolf–Rayet galaxies. They conclude that the nowadays best suitable method for star-forming galaxies, where auroral lines such as [O III] λ4363 Å are not observed, is Pilyugin

& Thuan (2005), and that other methods based on photoionization models yield metallicities systematically 0.2–0.3 dex higher and higher dispersion than the Pilyugin & Thuan (2005) calibration.

3.2 Determination of the stellar metallicities

Then, we determined the metallicity of the stellar content, i.e. of the stellar populations making up the galaxies, using a population synthesis method, described in Cuisinier et al. (2006) and Lisker et al. (2006), based on the full spectral fitting in the 3820–8570 Å range, whereas the upper limit can be lower than 8570 Å (in some rare cases as low as 7200 Å), where the deredshifted SDSS spectra do not extend up to this value.

As opposed to the method used for the determination of the line intensities, for this population synthesis we used SSP spectra from the so-called 'BC99' SSP library (Westera et al. 2004; Cuisinier et al. 2006; Lisker et al. 2006). It was produced using the GISSEL code, implementing the Padova 2000 isochrones (Girardi et al. 2000) combined with the BaSeL 3.1 'Padova 2000' stellar library (Westera 2001; Westera et al. 2002). The BaSeL 3.1 library was calibrated to reproduce the spectral shapes of stars of metallicities [Fe/H] from -2 to 0, so it is the ideal choice for full spectral fitting. By contrast, the 'BC03' library described in the previous section would not have been a good choice, for the reasons mentioned there. As the GISSEL spectra do not include nebular continuum emission, we added it to the spectra, in the same way as described in Westera et al. (2004), Cuisinier et al. (2006) and Lisker et al. (2006).

In Westera et al. (2004), we found that the stellar content of H II galaxies is made up of at least three populations, a young one (up to 10 Myr old) that is responsible for the ionization of the gas and, therefore, for the nebular emission, an intermediate one (from 20 to 500 Myr), and an old one (at least 1 Gyr old). We showed that these three populations are necessary – and sufficient – to characterize an H II galaxy, which is now the current view (Hoyos et al. 2007). Therefore, in this work we modelled the actual population as being composed of an old, an intermediate and a young stellar population. In a full spectral fit, we determined the masses, ages and metallicities of these partial populations. To obtain meaningful results, we chose to reduce the number of fitting parameters (and thus of degeneracies) to a minimum.

As the young population should be more or less coeval with the gas, whose metallicity is the one attained now by these galaxies, we assumed the young and intermediate populations to have the same chemical composition as the gas. As the gas metallicities we measured are in terms of [O/H], whereas our stellar population library was calibrated in [Fe/H], we still had to translate the oxygen into iron abundances, since the element ratios in H II galaxies are far from solar. Oxygen is released by stellar winds and by SNe I and II, whereas iron and other iron-peak elements are only produced in SNeIa, which appear only around 1 Gyr after the formation of a stellar population. Therefore, the ratio between the abundances of these two elements in a galaxy depends on its entire star formation history. Adding to this the possibility of 'selective mass loss', as is predicted by the models mentioned in the introduction, it would be illusory to expect a unique iron-to-oxygen ratio for the galaxies of our sample. However, as our sample is very homogeneous, we do expect there to exist a mean relation and only a moderate scatter around this relation. Unfortunately, transformations between the two metallicity indicators for H II galaxies are rare in the literature. In earlier abundance studies of this type of galaxies, such as Kniazev et al. (2004) and Izotov et al. (2006), the iron abundance is not determined, as they are also based on emission lines in SDSS spectra. On the other hand, most theoretical transformations, like the ones determined for the Milky Way bulge and the solar neighbourhood by Matteucci et al. (1999), are not valid for H II galaxies. Finally, we derived the [O/Fe] to [Fe/H] relation from the one for irregular galaxies from Calura et al. (2009), who calculated the element ratios of galaxies of different morphological types using chemical evolution models. According to their fig. 13, the [O/Fe] to [Fe/H] relation for irregular galaxies is around $[\mathrm{O/Fe}] = -0.25 \times [\mathrm{Fe/H}] - 0.425 \pm 0.15$ independent of redshift, which translates to $[\mathrm{Fe/H}] = 1.333 \times [\mathrm{O/H}] + 0.5666 \pm 0.2$. Hence, we fixed the metallicities of the young and intermediate populations, $[\mathrm{Fe/H}]_\mathrm{y}$ and $[\mathrm{Fe/H}]_\mathrm{i}$, to

$$[\mathrm{Fe/H}]_\mathrm{y} = [\mathrm{Fe/H}]_\mathrm{i} = 1.333 \times [\mathrm{O/H}]_\mathrm{P} + 0.5666. \quad (3)$$

For the galaxies of our sample, most of which have $[\mathrm{O/H}]_\mathrm{P}$ values in the range from -1 to -0.5, we obtain [O/Fe] ratios between -0.2 and -0.4. As opposed to the metallicity of the young and intermediate populations, the metallicity of the old population, $[\mathrm{Fe/H}]_\mathrm{o}$, is a free parameter of our fitting procedure, limited to the metallicities of the spectra of the 'BC99' SSP library, -2.252, -1.65, -1.25, -0.65, -0.35, 0.027 and 0.225. Contrary to our approach in previous works, we did not force the metallicities of the old populations to be lower than the ones of the younger stars, since one of the aims of this work is to verify if they really are.

As the decomposition of galaxy spectra into SSP spectra is known to present various degeneracies, we verified if our fitting procedure is able to recover the population parameters of synthetic composite spectra made up of three SSPs with noise added. We found that the masses, ages and metallicities of the input populations were properly recovered for the S/N values of both our H II galaxy sample and our test sample ($\geq$8 and 5 respectively in the g band), and conclude that the number of free parameters of our procedure is adequate and that the results presented in the following can be trusted to be meaningful.

In order to determine the total stellar masses of our galaxies, we had to know their luminosity distances D_L, and their (stellar) mass-to-light ratios. We calculated the former from the redshifts given by the SDSS, using a cosmology of $\Omega_\mathrm{m} = 0.3$, $\Omega_\Lambda = 0.7$ and $H_0 = 70\,\mathrm{km\,s^{-1}\,Mpc^{-1}}$. The stellar mass-to-light ratios result from our best fits.

4 RESULTS

The strengths of the emission lines used for this analysis, as well as the internal reddening values $E(B-V)$, the gas metallicities $[\mathrm{O/H}]_\mathrm{P}$ and the total stellar masses, M_tot, can be found in Table A1 with the electronic version of this paper (see Supporting Information).

Fig. 4 shows the stellar mass and gas metallicity distributions of our sample (in black) and the test sample (in grey). The average of the logarithms of the stellar masses (in $\mathrm{M}_\odot$) amounts to 9.4 and the average gas metallicity to -0.79, whereas those values are 9.8 and -0.78 respectively for the test sample.

As expected, the galaxies of the H II galaxy sample have, on average, lower masses than the ones of the test sample. Since our sample contains very few galaxies with stellar masses below $2 \times 10^8\,\mathrm{M}_\odot$ or above $2 \times 10^{10}\,\mathrm{M}_\odot$ (the mass bins at 5×10^6, 1×10^7, 2×10^7, 5×10^7, 1×10^8; 5×10^{10}, 1×10^{11}, 2×10^{11}, 5×10^{11} and $1 \times 10^{12}\,\mathrm{M}_\odot$ contain 1, 0, 4, 2, 3; 1, 2, 0, 0 and 0 galaxies, respectively), statistical studies of galaxies in these mass ranges suffer from low number statistics. In the following we will only consider the range from 2×10^8 to $2 \times 10^{10}\,\mathrm{M}_\odot$ when studying galaxy properties as a function of mass. In Figs 7 and 8, this mass range is delimited by dotted lines. For the test sample, the mass

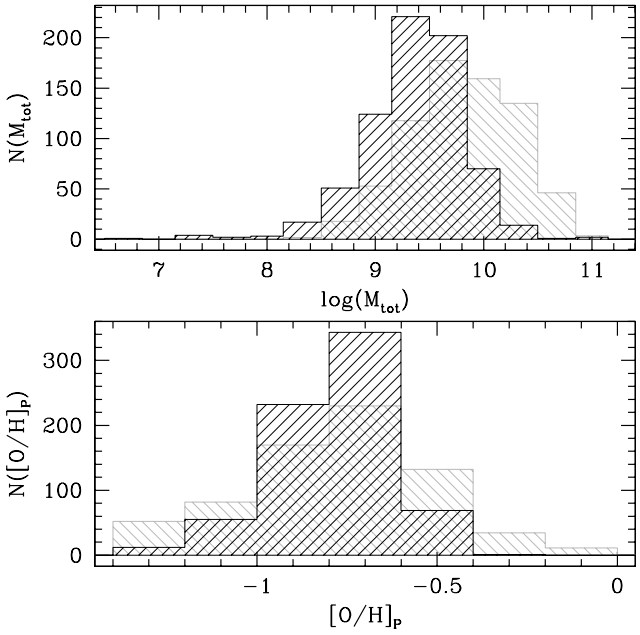

Figure 4. Stellar mass (top panel) and gas metallicity (bottom panel) distributions of the galaxies of our sample (in black). The mass and gas metallicity distributions of the test sample are shown in grey (scaled to the same total number of galaxies).

range from 2×10^8 to 1×10^{11} $M_\odot$ could be used for such studies, as each mass bin contains over 150 galaxies.

The average gas metallicities are nearly the same for both samples, but the distribution is narrower for the H II galaxies, indicating that this is a more homogeneous sample.

Fig. 5 shows the metallicity distributions of the partial populations. As we fixed $[Fe/H]_y = [Fe/H]_i = 1.333 \times [O/H]_P + 0.5666$ in the fitting procedure, we show in the upper panel the metallicity of the joint young- and intermediate-age population. The average metallicity of the joint young and intermediate populations is −0.49, and of the old one −0.87 (test sample: −0.49 and −0.84). Here too, the distributions are narrower for the more homogeneous H II galaxies sample. Nevertheless, the spread in $[Fe/H]_o$ is wide. As $[Fe/H]_o$ is a measure of the average metallicity of all populations older than ∼1 Gyr, this wide spread reflects the various stages of (metallicity) evolution of the galaxies of our sample around 1 Gyr ago.

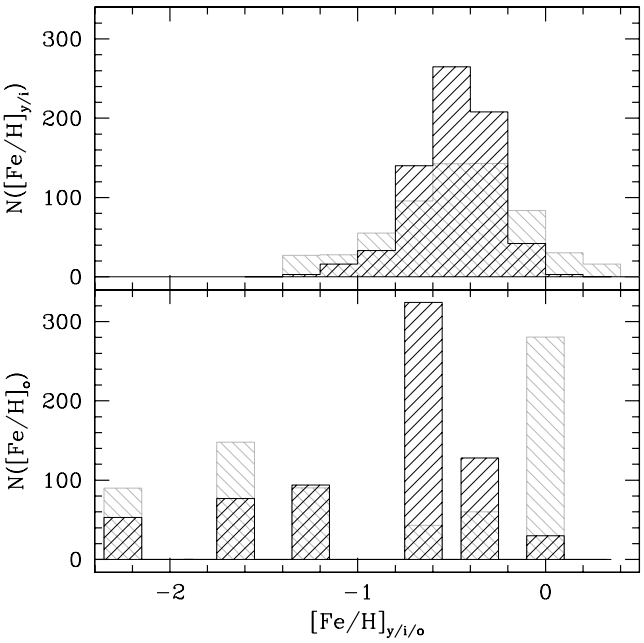

Figure 5. Metallicity distributions of the partial populations in our galaxy sample. Top panel: the joint young- and intermediate-age populations. Bottom panel: old populations. The metallicity distributions of the partial populations in the test sample are shown in grey (scaled to the same total number of galaxies).

5 DISCUSSION

In Fig. 6, we show the gas metallicity in function of the metallicity of the old population, both for the H II galaxies and for the test sample. In either sample, not much of a relation can be seen, any possible trend being significantly smaller than the scatter. Apparently, the stage of a galaxy's evolution around 1 Gyr ago is not necessarily reflected in the present-day one. The chemical evolution and the present-day (gas) metallicities of galaxies suffer stronger influences from other factors, such as the galaxy mass.

Fig. 7 shows how the present gas metallicity $[O/H]_P$ depends on the total stellar galaxy mass. In the test sample, $[O/H]_P$ clearly increases with mass in the range from 2×10^8 to 1×10^{11} $M_\odot$, as has been found in previous studies (Tremonti et al. 2004; Thomas et al. 2005; Asari et al. 2007; Panter et al. 2008, and others). However, our mass–metallicity relation lies lower than the ones found in these works, as recent studies (Ellison et al. 2008; Mannucci et al. 2010) suggest to be the case for samples of star-forming galaxies, such as our test sample.

The H II galaxy sample represents galaxies of a more homogeneous class than the test sample. Therefore, in this sample, the mass–metallicity relation is much less pronounced, if existing at all. In fact, the average gas metallicity stays constant between −0.7 and −0.8 in the full galaxy mass range from 2×10^8 to 2×10^{10} $M_\odot$. Panter et al. (2008) find almost the same relation for their subsample

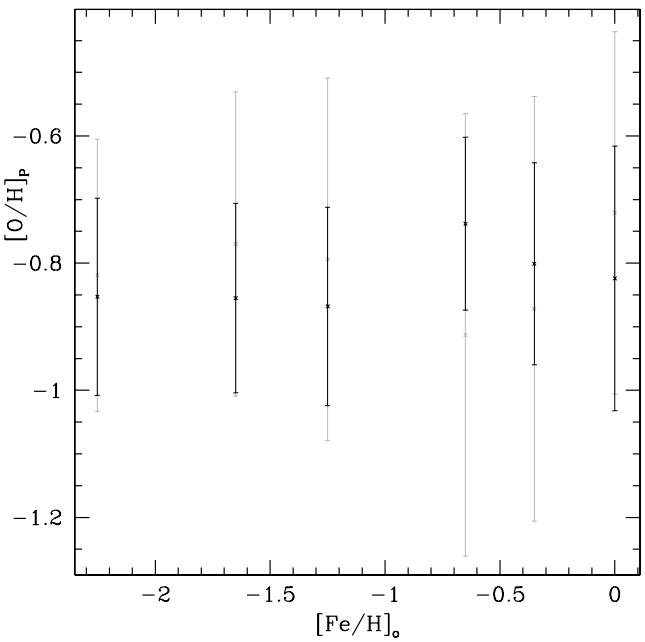

Figure 6. Gas metallicities as a function of the metallicities of the old populations. The crosses represent the average of the gas metallicities for each old population metallicity value, and the error bars show the standard deviations.

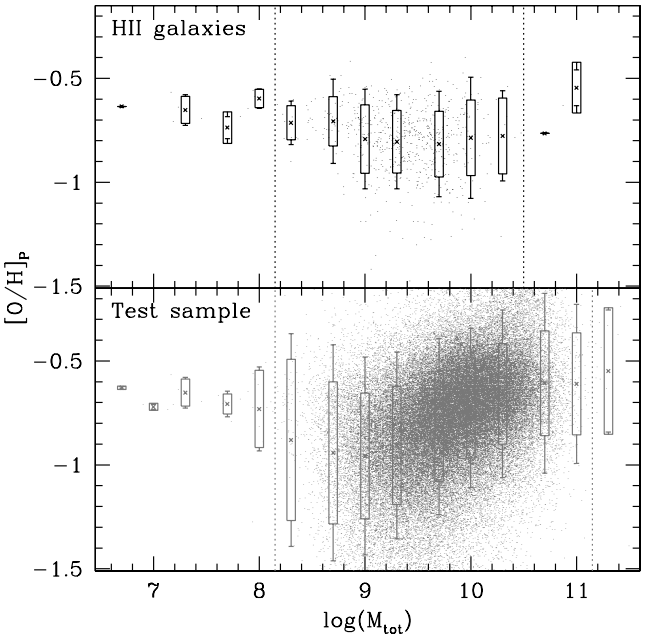

Figure 7. Top panel: the gas metallicity $[O/H]_P$ as a function of the total stellar mass of the galaxies of our sample. The dots show the individual galaxies, whereas the crosses, boxes and bars show the statistical properties after subdividing the sample into mass bins. For each value of M_{tot}, the crosses represent the average, the boxes represent the standard deviation and the vertical bars represent the 90th percentile range. The dotted vertical lines detach the 'trustworthy' range from the nearly empty mass bins. Bottom panel: the individual galaxies, average, standard deviation and 90th percentile range of $[O/H]_P$ for the test sample.

of galaxies that are (flux-)dominated by young populations ($\leq$0.5 Gyr), as can be seen in their fig. 10.

In a 'closed box' context, this would mean that the gas fraction that has been transformed into stars so far is in the same range for all galaxies of the H II galaxy sample, independent of their masses. However, H II galaxies are not 'closed boxes', and our results should be interpreted in the light of models including interaction processes with the environment, like the ones presented in Section 1.

Most of these models predict that H II galaxies lose a large fraction of their heavy elements through galactic winds, whose escape efficiencies depend upon the galaxy mass. These models are at odds with our result for two reasons: they result in a dependence of the metallicity on the galaxy mass and their predicted present-day metallicities are lower than the ones we measure.

The Recchi et al. (2006) and Recchi & Hensler (2007) models with constantly infalling clouds appear more promising, especially the models NGC-4+BC of Recchi et al. (2006) and NCSM of Recchi & Hensler (2007). The clouds partially retain the metal-rich gas, resulting in higher present-day metallicities. Depending on the star formation history and on the mass of the infalling clouds, galaxies like the ones described in these models can reach the metallicities we measure. On top of that, this scenario provides a possible explanation, why we find metallicities in the same ranges for different stellar masses. Not only the SFR and, therefore, the amount of produced metals and galactic wind increase with increasing galaxy mass, but also the amount of infalling low-metallicity clouds and of retained outflowing high-metallicity gas. Of course, only detailed model calculations can tell, if the mass dependencies of the different metallicity-increasing and -decreasing processes really add up in such a way, that the final metallicity becomes mass-independent. The fact that a constant mass–metallicity relation is observed only in our H II galaxy sample and not, for example, in our test sample, or in any of the studies mentioned at the beginning of this section, shows that only in galaxies with extreme star formation, and thus extreme stellar winds, the metal outflow manages to balance the retention in this way. However, the models including infalling clouds seem to be on the right track.

Another noteworthy point of Fig. 7 is that though the average gas metallicity $[O/H]_P$ does not vary with the galaxy mass, its dispersion does increase with galactic mass. This indicates that high-mass galaxies have a more complex chemical, and certainly assembly, history.

Apart from the present-day metallicity, our analysis also allows us to quantify the chemical evolution of our sample galaxies since the formation of the old population. As the metallicity of the young (and intermediate) population represents the galaxy's present-day metallicity, and the one of the old population is a measure of the average metallicity of all stars older than $\sim$1 Gyr, the quantity $[Fe/H]_{y/i} - [Fe/H]_o$, which we shall call the metal enrichment, is a good measure of the change in metallicity during the last few Gyr. Fig. 8 shows the metal enrichment in function of the stellar mass for the galaxies in both our H II galaxies sample and the test sample. For our H II galaxies, the enrichment is fairly constant of the order of 0.3 up to $5 \times 10^9\,M_\odot$, and almost 0.5 dex higher for the last two mass bins within the mass range, where reliable statistics are possible, 1×10^{10} and $2 \times 10^{10}\,M_\odot$. This suggests that the enrichment mechanism is independent of mass up to $5 \times 10^9\,M_\odot$, which is compatible with the formation scenario favoured in the previous paragraph. For galaxy masses above $5 \times 10^9\,M_\odot$, the enrichment is significantly higher, which means that at high

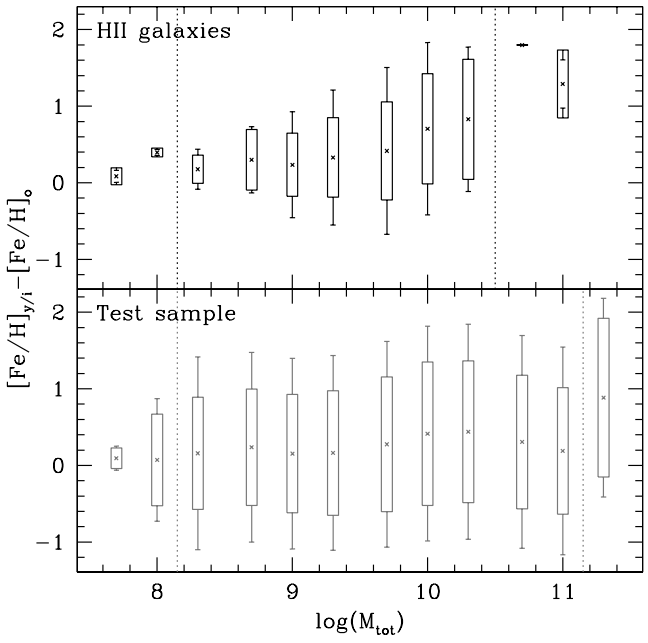

Figure 8. Top panel: the metal enrichment, $[Fe/H]_{y/i} - [Fe/H]_o$, as a function of the total mass of the galaxies of our sample. For each value of M_{tot}, the crosses represent the average, the boxes represent the standard deviation and the vertical bars represent the 90th percentile range. The dotted vertical lines detach the 'trustworthy' range from the nearly empty mass bins. Bottom panel: the average, standard deviation and 90th percentile range of $[Fe/H]_{y/i} - [Fe/H]_o$ for the test sample.

masses, the metal-rich gas could not escape the galaxy's potential well, as predicted in the MacLow & Ferrara (1999) models. Here too, the dispersion increases with galaxy mass, confirming more complex chemical and assembly histories for high-mass galaxies.

An interesting point is that we find a negative metal enrichment, thus a metal reduction, for 164 galaxies, i.e. 23 per cent of our sample. Two mechanisms are known to reduce the (gas) metallicity of a galaxy: selective outflow of metal-enriched gas and infall of low-metallicity gas clouds, maybe even of primordial composition. Both processes might have contributed to the metal reduction of our galaxies, but in the light of our previous results, we expect the second one to be more important on long time-scales.

It is intriguing that in the test sample, too, we find the metal enrichment to be mass-independent, even though the final metallicity increases with galaxy mass. $[Fe/H]_{y/i} - [Fe/H]_o$ amounts to around 0.36 in the full range from 2×10^8 to $1 \times 10^{11}\,M_\odot$. Even the dispersion is fairly constant over this mass range. Apparently, enrichment mechanisms are similar for galaxies of different masses even in a heterogeneous sample like our test sample. Around 44 per cent of the test sample galaxies, 33 178 in total, show negative metal enrichment, which proves that processes like selective outflow or low-metallicity gas infall are also at play in these galaxies.

6 CONCLUSIONS

We performed a gas and stellar population analysis of H II galaxies from the SDSS Data Release 7, using their full spectra. We selected a sample which contains 712 H II galaxy spectra, a relatively low number due to our high requirements towards the quality of the spectra and to the criterion that the spectra contain all the spectral lines necessary for our study. We also selected a test sample of 74 989 galaxies, using less restrictive requirements, the only criterion being that they show some line emission. Therewith, it is a sample of star-forming galaxies.

We derived independent metallicities for the young populations present in our sample galaxies from the gas emission lines, and for the old populations from full spectra fitting, i.e. from the continuum and absorption features from stars.

Our test sample follows the well-known mass–metallicity relation, e.g. the fact that the (gas) metallicity increases with (stellar) galaxy mass, indicating that low-mass galaxies are chemically less evolved than high-mass galaxies. We do not find any systematical tendency of the difference between the metallicities of the young and the old stellar populations, a quantity we call metallicity enrichment, with galactic mass, indicating that, on average, recycling mechanisms of the interstellar medium should be the same for low- and high-mass galaxies.

In our H II galaxy sample, on the other hand, we find no mass dependence of the present-day metallicity. For the metallicity enrichment, we find no mass dependence for masses up to $5 \times 10^9\,M_\odot$, whereas above this mass, the enrichment is significantly higher.

We interpret these findings in the light of recent hydrodynamical evolutionary models of dwarf irregular galaxies, of which H II galaxies are a subclass. We favour models featuring constantly infalling low-metallicity clouds able to retain part of the high-metallicity galactic winds, such as the models NGC-4+BC from Recchi et al. (2006) and NCSM from Recchi & Hensler (2007), since models without infalling clouds fail to predict the metallicities and the non-dependence on galaxy mass of our sample galaxies. For galaxies with masses above $5 \times 10^9\,M_\odot$, most, if not all, of the metal-rich gas is retained by the galaxy's gravitational potential, as predicted by MacLow & Ferrara (1999), which leads to the observed breakdown of the constant mass–enrichment relation.

However, the dispersion of both the present-day metallicity and the metallicity enrichment does increase with galactic mass, indicating more complex chemical and assembly histories for high-mass H II galaxies.

In 23 per cent of our H II galaxies, the metallicity has decreased in the last few Gyr. We attribute the metallicity decrease mainly to the dilution of the galactic gas by the infalling clouds, which is compatible with the models we favour.

ACKNOWLEDGMENTS

We would like to thank the Fundação Carlos Chagas Filho de Amparo à Pesquisa do Estado do Rio de Janeiro (FAPERJ) and the PCI programme of ON/MCT (DTI/CNPq) for financial support. We would like to thank as well Eduardo Telles and Helio Rocha-Pinto for fruitful discussions. Finally, the authors acknowledge support by the Swiss National Science Foundation.

REFERENCES

Abazajian K. N. et al., 2009, ApJS, 182, 543
Asari N. V., Cid Fernandes R., Stasińska G., Torres-Papaqui J. P., Mateus A., Sodré L., Schoenell W., Gomes J. M., 2007, MNRAS, 381, 263
Baldwin J. A., Phillips M. M., Terlevich R., 1981, PASP, 93, 5
Bruzual A. G., Charlot S., 1993, ApJ, 405, 538
Bruzual A. G., Charlot S., 2003, MNRAS, 344, 1000
Calura F., Pipino A., Chiappini C., Matteucci F., Maiolino R., 2009, A&A, 504, 373
Calzetti D., 2001, PASP, 113, 1449
Calzetti D., Kinney A. L., Storchi-Bergmann T., 1994, ApJ, 429, 582
Charlot S., Bruzual A. G., 1991, ApJ, 367, 126
Cid Fernandes R., Leão J. R. S., Lacerda R. R., 2003, MNRAS, 340, 29
Cid Fernandes R., Asari N. V., Sodré L., Jr, Stasińska G., Mateus A., Torres-Papaqui J. P., Schoenell W., 2007, MNRAS, 375, L16
Cuisinier F., Westera P., Telles E., Buser R., 2006, A&A, 423, 133
Denicoló G., Terlevich R., Terlevich E., 2002, MNRAS, 329, 315
Ellison S. L., Patton D. R., Simard L., McConnachie A. W., 2008, ApJ, 672, L107
Fagotto F., Bressan A., Bertelli G., Chiosi C., 1994, A&AS, 105, 39
Fitzpatrick E. L., 1999, PASP, 111, 63
French H. B., 1980, ApJ, 240, 41
Girardi L., Bressan A., Chiosi C., Bertelli G., Nasi E., 1996, A&AS, 117, 113
Girardi L., Bressan A., Bertelli G., Chiosi C., 2000, A&AS, 141, 371
Hägele G. F., Díaz A. I., Terlevich E., Terlevich R., Pérez-Montero E., Cardaci M. V., 2008, MNRAS, 383, 209
Hoyos C., Guzmán R., Díaz A. I., Koo D. C., Bershady M. A., 2007, AJ, 134, 2455
Izotov Y. I., Stasińska G., Meynet G., Guseva N. G., Thuan T. X., 2006, A&A, 448, 955
Kehrig C., Telles E., Cuisinier F., 2004, AJ, 128, 1141
Kehrig C., Vílchez J. M., Telles E., Cuisinier F., Pérez-Montero E., 2006, A&A, 457, 477
Kewley L. J., Dopita M. A., 2002, ApJS, 142, 35
Kewley L. J., Dopita M. A., Sutherland R. S., Heisler C. A., Trevena J., 2001, ApJ, 556, 121
Kniazev A. Y., Pustilnik S. A., Grebel E. K., Lee H., Pramskij A. G., 2004, ApJS, 153, 429
Kobulnicky H. A., Kewley L. J., 2004, ApJ, 617, 240
Kong X., Charlot S., Weiss A., Cheng F., 2003, A&A, 403, 877
Le Borgne J.-F. et al., 2003, A&A, 402, 433
Lequeux J., Peimbert M., Rayo J. F., Serrano A., Torres-Peimbert S., 1979, A&A, 80, 155
Lisker T., Glatt K., Westera P., Grebel E. K., 2006, AJ, 132, 2432

López-Sánchez Á. R., Esteban C., 2010, A&A, 517, A85
McGaugh S. S., 1991, ApJ, 380, 140
MacLow M.-M., Ferrara A., 1999, ApJ, 513, 142
Mannucci F., Cresci G., Maiolino R., Marconi A., Gnerucci A., 2010, MNRAS, 408, 2115
Matteucci F., Romano D., Molaro P., 1999, A&A, 341, 458
Osterbrock D. E., 1989, Astrophysics of Gaseous Nebulae and Active Galactic Nuclei. University Science Books, Mill Valley, CA
Pagel B. E. J., Edmunds M. G., Blackwell D. E., Chun M. S., Smith G., 1979, MNRAS, 189, 95
Panter B., Jimenez R., Heavens A. F., Charlo S., 2008, MNRAS, 391, 1117
Pérez-Montero E., Díaz A. I., 2003, MNRAS, 346, 105
Pérez-Montero E., Díaz A. I., 2005, MNRAS, 361, 1063
Pérez-Montero E., García-Benito R., Hägele G. F., Díaz A. I., 2010, MNRAS, 404, 2037
Pettini M., Pagel B. E. J., 2004, MNRAS, 348, 59
Pilyugin L. S., 2001a, A&A, 369, 594
Pilyugin L. S., 2001b, A&A, 374, 412
Pilyugin L. S., Thuan T. X., 2005, ApJ, 631, 231
Raimann D., Bica E., Storchi-Bergmann T., Melnick J., Schmitt H., 2000, MNRAS, 314, 295
Recchi S., Hensler G., 2007, A&A, 476, 841
Recchi S., Matteucci F., D'Ercole A., 2001, MNRAS, 322, 800
Recchi S., Matteucci F., D'Ercole A., Tosi M., 2002, A&A, 384, 799
Recchi S., Matteucci F., D'Ercole A., Tosi M., 2004, A&A, 426, 37
Recchi S., Hensler G., Angeretti L., Matteucci F., 2006, A&A, 445, 875
Sargent W. L. W., Searle L., 1970, ApJ, 162, L155
Schlegel D. J., Finkbeiner D. P., Davis M., 1998, ApJ, 500, 525
Searle L., Sargent W. L. W., Bagnuolo W. G., 1973, AJ, 179, 427
Tenorio-Tagle G., Muñoz-Tuñón C., Pérez E., Silich S., Telles E., 2006, ApJ, 643, 186
Terlevich R., Melnick J., Masegosa J., Moles M., Copetti M. V. F., 1991, A&AS, 91, 285
Thomas D., Maraston C., Bender R., Mendes de Oliveira C., 2005, ApJ, 621, 673
Tremonti C. A. et al., 2004, ApJ, 613, 898
Vílchez J. M., Iglesias-Páramo J., 2003, ApJS, 145, 225
Westera P., 2001, PhD thesis, Univ. Basel
Westera P., Lejeune T., Buser R., Cuisinier F., Bruzual A. G., 2002, A&A, 381, 524
Westera P., Cuisinier F., Telles E., Kehrig C., 2004, A&A, 423, 133
York D. G. et al., 2000, AJ, 120, 1579
Zaritsky D., Kennicutt R. C., Jr, Huchra J. P., 1994, ApJ, 420, 87

APPENDIX A: POPULATION PARAMETERS OF INDIVIDUAL SPECTRA

SUPPORTING INFORMATION

Additional Supporting Information may be found in the online version of this article:

Table A1. Line strengths, internal reddening, gas metallicities and total stellar masses of individual spectra.

Please note: Wiley-Blackwell are not responsible for the content or functionality of any supporting materials supplied by the authors. Any queries (other than missing material) should be directed to the corresponding author for the article.

Table A1. Line strengths, internal reddening, gas metallicities and total stellar masses of individual spectra (first 10 lines only; for the complete sample, see the Supporting Information with the electronic version of the paper).

SDSS spectroscopic ID MJD-plate-fibre	$I(\mathrm{H}\beta)^a$ 4861 Å	$\mathrm{H}\alpha^b$ 6563 Å	$[\mathrm{O\,II}]^b$ 3727 Å	$S/N_{[\mathrm{O\,II}]}$ 3727 Å	$[\mathrm{O\,III}]^b$ 4959 Å	$[\mathrm{O\,III}]^b$ 5007 Å	$[\mathrm{N\,II}]^b$ 6548 Å	$[\mathrm{N\,II}]^b$ 6584 Å	$E(B-V)$	$[\mathrm{O/H}]_\mathrm{P}$	M_tot $[10^9\,\mathrm{M}_\odot]$
51637-0306-583	5.102	3.010	5.848	2.948	0.728	2.088	0.148	0.472	0.088	−1.022	0.63
51658-0282-047	10.075	3.103	5.644	2.806	0.694	2.049	0.143	0.457	0.145	−0.991	1.93
51662-0308-628	10.264	3.017	4.800	4.074	0.669	2.049	0.158	0.571	0.093	−0.860	2.11
51663-0307-268	14.076	3.052	4.270	3.005	1.009	3.078	0.176	0.574	0.114	−0.794	3.27
51671-0299-571	8.794	3.179	6.656	2.846	0.615	2.199	0.203	0.626	0.189	−1.142	6.78
51691-0350-439	24.324	3.105	3.533	3.102	0.550	1.696	0.212	0.644	0.146	−0.654	1.98
51692-0339-437	11.115	2.921	2.707	4.272	1.238	3.741	0.074	0.223	0.033	−0.599	0.34
51783-0395-570	9.257	2.924	3.362	4.199	0.639	1.975	0.118	0.374	0.034	−0.624	0.98
51812-0404-507	9.680	3.042	4.195	3.339	0.641	1.964	0.144	0.490	0.108	−0.763	4.10
51818-0383-266	8.743	2.944	3.631	3.398	0.899	2.789	0.097	0.303	0.047	−0.687	0.87

[a] $I(\mathrm{H}\beta)$ given in units of 10^{15} erg s^{-1} cm^{-2}.
[b] Flux ratios given in $I(\lambda)/I(\mathrm{H}\beta)$.

This paper has been typeset from a TEX/LATEX file prepared by the author.